Journal of American Science

Websites:
http://www.jofamericanscience.org
http://www.sciencepub.net

Emails:
editor@sciencepub.net
sciencepub@gmail.com

MARSLAND PRESS
Multidisciplinary Academic Journal Publisher

Effect of Exogenous Stem Cells versus Mobilization of Endogenous Stem Cells on the Nonalcoholic Fatty Liver of Adult Male Albino Rat (Histological and Immunohistochemical Study)

Asmaa Azzam, Emad S. Mishriki, Aml Abo Elala and Fotna Eskander

Department of Anatomy, Faculty of Medicine, Tanta University, Egypt
E-mail addresses: asmaa.azzam@med.tanta.edu.eg
emad.mishriki@med.tanta.edu.eg

Abstract: Introduction: Nonalcoholic fatty liver diseases are currently the most common chronic liver disease. Mesenchymal stem cells have been approved for their hepatoprotective effect and as a substitute for liver transplantation. Stem Enhance (SE) is a hematopoietic stem cell mobilizer which has antioxidant and cholesterol-regulatory effects. **Material and methods:** Sixty adult male albino rats were used. Ten rats were used for preparation of stem cells. For ten weeks, fifty rats were divided into control and experimental groups. Group-I (Control) was twenty rats divided into two equal subgroups: Ia (negative control) and Ib (SE control). Group-II (Experimental) was thirty rats received high fatty diet (HFD) and after six weeks they subdivided into three equal subgroups: IIa (HFD with no treatment), IIb (SE treated) and IIc (BM-MSCs treated). Body weight, liver enzymes and serum lipids were measured. Liver specimens were stained using different histological and immunohistochemical techniques. **Results:** Subgroup IIa showed enlarged yellowish liver with disturbed architecture, marked steatosis, inflammatory cells and fibrosis with highly significant increase in the mean level of serum lipids and liver enzymes. Subgroup IIb showed moderate restoration of hepatic architecture with mild distribution of steatosis and fibrosis was decreased. Subgroup IIc revealed restored normal hepatic architecture with mild steatosis and markedly diminished fibrosis. Liver enzymes and serum lipids were decreased in subgroups IIb and IIc at different degrees. **Conclusion:** It could be concluded that exogenous bone marrow derived stem cell transplantation presents a better therapeutic approach for the nonalcoholic fatty liver diseases as compared to mobilization of endogenous stem cells using Stem Enhance.

[Asmaa Azzam, Emad S. Mishriki, Aml Abo Elala and Fotna Eskander. **Effect of Exogenous Stem Cells versus Mobilization of Endogenous Stem Cells on the Nonalcoholic Fatty Liver of Adult Male Albino Rat (Histological and Immunohistochemical Study).** *J Am Sci* 2019;15(12):122-138]. ISSN 1545-1003 (print); ISSN 2375-7264 (online). http://www.jofamericanscience.org. 14. doi:10.7537/marsjas151219.14.

Key words: NAFLD, BM-MSCs, Stem Enhance, exogenous stem cells, endogenous stem cells.

1. Introduction

Nonalcoholic fatty liver disease (NAFLD) is defined as the presence of fat in the liver (hepatic steatosis) affecting more than 5% of hepatocytes either on imaging or on liver histology after the exclusion of secondary causes of fat accumulation in the liver. NAFLD is further categorized histologically into nonalcoholic fatty liver (NAFL) and nonalcoholic steatohepatitis (NASH) ***(McPherson et al., 2015).***

NAFLD is a major potential threat to public health and is considered one of the most prevalent liver diseases today. It affects at least 30 % of the general population and is present in more than 60 % of obese subjects. The increased prevalence of NAFLD is strongly associated with the increasing prevalence of obesity. Patients who are diagnosed as NAFLD have a significantly higher risk of diabetes, cardiovascular disease and liver-related mortality ***(Loomba and Sanyal, 2013)***.

Dietary modification has important benefits for management of NAFLD. However, other metabolic risk factors require further treatment. Despite considerable research and multiple clinical trials, no single pharmacologic agent has been achieved for treatment of NAFLD. Currently, there is a wide variety of compounds with a different mode of actions in clinical development. It is most likely that a combination therapy is needed. ***(Filozof et al., 2015)***.

Bone marrow mesenchymal stem cells are multipotent cells which have the ability for differentiation into a variety of cells including functional hepatocyte-like cells. Benefits of stem cell-based therapies include down-regulation of immune mediated liver damage, augmenting liver function, counteracting progressive organ fibrosis and subsequently improving scarring which could be a promising strategy for patients with liver failure and cirrhosis ***(Kallis et al., 2007 & Zhang and Wang, 2013)***.

Stem Enhance (SE) is a haematopoietic stem cell mobilizer extracted from Aphanizomenonflos-aquae which has been proved to have a hepatoprotective effect. This effect is mediated by the mobilization of hematopiotic stem cells that possibly induce hepatic restoration and exert paracrine effects on hepatic inflammatory and fibrotic damage ***(El-Akabawy and El-Mehi, 2015 & Osman, 2016)***.

2. Material and Methods

2.1. Animals & experimental design

This experimental study was done using 60 adult male Sprague-Dawley albino rats with average weight (180-200 gm /each). All animals were kept in clean properly ventilated separate metal cages under the same environmental conditions. The animals had free access to water and standard food two weeks before starting the experiment. **10** rats were used to obtain bone marrow derived mesenchymal stem cells. **50**rats were randomly separated into two major groups: control group and experimental group as follows:

Control group (Group I): This group consisted of 20 rats which were divided into 2 subgroups as follows:

- **Subgroup Ia (negative control)**: It consisted of 10 rats. They were fed standard rat diet for 10 weeks and received no treatment.
- **Subgroup Ib (SE control):** It consisted of 10 rats. They were fed standard rat diet for 10 weeks and received SE at the start of the 7thweek till the end of 10th week.

Experimental group (Group II):

This group consisted of 30 rats. They were fed high fat diet (HFD) for 6 weeks. The HFD was prepared every two days and consisted of: 70% rat chow, 25% lamb fat, 2% sesame oil and 3% butter ***(Lau et al., 2016)***. Then rats were randomly separated into 3 subgroups (10 rats / each subgroup) as follows:

- **Subgroup IIa (10 weeks HFD)**: The rats were fed high fat diet for further 4 weeks then sacrificed.
- **Subgroup IIb (SE treated)**: The rats continued to be fed high fat for another 4 weeks, while they received SE orally from the start of 7th week till the end of 10th week then rats were sacrificed.
- **Subgroup IIc (BM-MSCs treated)**: The rats received BM-derived MSCs (3×10^{6} BM-MSCs suspended in 0.5 ml phosphate buffer solution) at the start of the 7th week as a single dose intra-hepatic via the portal vein. These rats continued on fatty diet for further 4 weeks then sacrificed ***(Kim et al., 2010)***.

2.2. Drug used

Stem Enhance (SE):

SE capsules are a product of STEM Tech Health Sciences (San Clemente, CA, USA). The bottle contained 50 hard capsules. Each capsule contained 500 mg of L-selectin ligand enriched fractions of AFA. SE was solubilized in distilled water and given using a gastric tube at a dose of 270 mg/kg per day once daily for 4 successive weeks ***(Ismail et al., 2015)***.

2.3. Bone marrow-derived mesenchymal stem cells (BM-MSCs)

a) Bone marrow isolation: ***(Yusop et al., 2018)***

The rats were anesthetized by diethyl ether inhalation and sacrificed. Skin over hind limbs was shaved and aseptically prepared for dissection. The skin was incised along the lateral aspect of the both thighs and legs. Tibia and femur were extracted after removing the muscular and tendinous attachment then placed separately in a 50 ml centrifuge tube containing phosphate buffer solution (PBS) and antibiotics. The bones were then placed under laminar hood in Petri dish containing high-glucose Dulbecco's modified Eagle's medium with antibiotics. After removal of the epiphysis of both ends of bones, the bone marrow was flushed out from the medullary cavity using a gauge-needle with 2 ml of complete media to obtain cell suspension. This suspension was then filtered by a filter mesh to remove any bone spicules or muscle. The marrow extract was received in sterile tissue culture tubes and immediately processed for mesenchymal stem cell isolation and culture.

b) BM-MSCs isolation and culture: ***(Karaoz et al., 2009)***

Marrow plug suspension was centrifuged for 10 min to obtain cell pellet and the supernatant containing thrombocytes and erythrocytes was discarded. Then 3ml of complete media was added to the cell pellet and gently rapped till dissolved and full suspension was obtained.20 ml of preformed complete media was added to the cells from this suspension in a tissue culture flask. Then the flask was incubated at 37°C in a humidified atmosphere containing 5% CO2 and 95% air. After an additional 8 h of culture, the medium was replaced with 1.5 ml of fresh complete medium. This step was repeated every 8 h for up to 72 h of initial culture. Examination using inverted microscope was done to follow up the growth of the cells and exclude any infection in the culture. On the 6th day, red blood cells and other non-adherent cells were removed. Adherent cells were then washed twice with a sterile PBS and fresh medium was added to the flask to allow further growth. The medium was exchanged every three days and replaced with 10 ml of pre-warmed complete media. After 2 weeks (14 days) of initiating culture, cells reached a confluence of 70-80% and monitored by inverted microscopy. The cells were defined as passage zero (P0) cells. The P0 MSCs were washed with PBS and detached by

incubation with 0.25% Trypsin / Ethylene diamine tetra acetic acid solution for 5–10 min at 37°C. Trypsin was then neutralized by adding 5 ml of pre-warmed complete medium. Detached cells were transferred to 15 ml conical tube and centrifuged for 5 minutes and the supernatant was removed then the cells obtained were suspended in a small amount of pre-warmed complete media. The viability of the prepared stem cells was assessed by cell counting using Trypan-Blue.

c) Labeling of BM-MSCs with green fluorescent protein (GFP): ***(Guo et al., 2012 & Gabr et al., 2015)***

To ensure healthy cells prior to transduction, the culture medium was changed when the BM-MSCs had reached 60% confluence. The medium containing 10% fetal bovine serum (FBS) was removed prior to transduction. In vitro GFP labeling was done by adding plasmid cytomegalovirus Aequoreacoerulescens green fluorescent protein (pCMV-AcGFP) mixed with lipofectamine at a 2:1 ratio to each plate and incubating at 37°C for 6 h before transplantation. The flask was shaken gently every 15 min for 2 h. After incubation with pCMV-AcGFP for 2 h, culture medium containing 10% FBS was added into the flask. BM-MSCs labelled with GFP were observed in the liver sections of subgroup IIc four weeks after intraportal injection using Fluorescence Microscope.

d) Intraportal injection of BM-MSCs: ***(Wang et al., 2012 & Goddard et al., 2016)***

After anesthesia, the rat was placed in a supine position. A single 1-2 inch incision was made into the skin at a sagittal plane starting just below the ribs and ending just above the plane of the fourth inguinal mammary gland. A similar 1-inch incision was done into the peritoneum **(fig. 1-A)**. The large and small intestines were carefully pulled out until the portal vein was visualized **(fig. 1-B)**. Internal organs were covered with saline soaked gauze to maintain internal moisture and sterility. The needle loaded with 3×10^6 BM-MSCs suspended in 0.5 ml PBS was inserted into the portal vein **(fig. 1-C)**. The needle was removed while simultaneously placing a sterile cotton tip applicator on the vein with pressure. Once the injection site is deemed intact, with no blood leaving the injection site, the internal organs were placed gently back into the abdominal cavity. The peritoneal lining and then the skin was sutured with sterile 4-0 vicryl suture. Injected rats were then kept in separate cages and continued on fatty diet for another 4 weeks.

2.4. Study Methodology:

2.4.1. Liver extraction and gross examination:

At the scheduled time, rats were anaesthetized then sacrificed. Livers of the control and experimental rats were carefully removed, washed with cold saline solution and dried then photographed for gross observation of color and surface.

2.4.2. Assessment of rat body weight:

Body weight for each rat was assessed at the end of the work. All data were collected and statistical analysis was performed.

2.4.3. Biochemical study:

Blood samples were taken at the end of the experiment. All rats were fasted overnight then blood samples were immediately collected from the retro-orbital plexus with capillary tubes into clean dried centrifuge tubes. The tubes were then centrifuged for15min. Clear serum samples were carefully separated using Pasteur pipettes and frozen at −20°C until biochemical analysis for assessment of the following:

a) Serum lipids: The serum levels of triglyceride (TG) and total cholesterol (TC) were assessed with standard techniques based on enzymatic and colorimetric methods, according to manufacturer's recommendations.

b) Liver enzymes: The serum level of alanine transaminase (ALT) and aspartate transaminase (AST) enzymes were assessed spectrophotometrically according to the routine biochemical analysis system using clinical test kits (Elitech, UK).

2.4.4. Histological study:

Each liver specimen was divided into two parts:

A- One part was fixed in 10% formal saline solution for preparation of paraffin blocks.

B- Another fresh part for Oil Red O staining.

A- Preparation of paraffin blocks:

The collected liver specimens were washed with normal saline solution and immediately fixed in 10% formol saline. The fixed specimens were then dehydrated in ascending grades of ethanol and then cleared in two changes of xylol. They were impregnated in pure soft paraffin for 2 hours at 55˚c followed by embedding them in hard paraffin blocks. Sections of 5-6 micron thickness were cut by the microtome and stained with the following stains:

I) Haematoxylin and Eosin (Hx. & E.)

II) Mallory trichrome.

III) Immunohistochemical (IHC) stains:

a) Tumor necrosis factor alpha (TNF-α)

b) Glial fibrillary acidic protein (GFAP)

I) Hx. & E. ***(Bancroft and Layton, 2013):***

H & E stain were used to study the general histological structure of rat's liver in all groups**.** The first step before staining is removal of wax from the slide by xylene. Sections need rehydration after dewaxing. This was done by putting the slides in descending series of alcohol from 90%, 70% to 50%. Then the slides were immersed in distilled water. The sections were stained in hematoxylin for 15 minutes and washed in tape water for 10 minutes. Then, they

were stained in eosin for 1 minute. After staining, the section was covered with a cover glass then the slides were allowed to dry for few minutes.

II) Mallory trichrome.

III) IHC stains:

a) TNF-α: ***(Fujimoto et al., 2012)***

Sections on coated slides were deparaffinized in xylene then taken through ethanol and rinsed in tap water to rehydrate. Endogenous peroxidase activity was blocked by incubating the sections in a solution of 3% hydrogen peroxide for 20 minutes at room temperature. Sections were immersed in antigen retrieval solution then washed with PBS for blocking of nonspecific protein binding. After washing in PBS the sections were incubated with the primary polyclonal anti rat-TNF-alpha 1:200 (Abcam, London, United Kingdom) overnight at 4°C. The sections were washed with PBS and incubated with a biotinylated secondary antibody for 30 minutes, followed by incubation with Avidin Biotin Complex (ABC)-Peroxidase solution for further 30 minutes at room temperature. Staining was carried out using a solution 3'diaminobenzidine (DAB) containing 1% hydrogen peroxide and lightly counterstained with Mayer's hematoxylin. Sections were rinsed in running tap water for 2-5 minutes, dehydrated through 95% ethanol for 1 minute and 100% ethanol for 3minutes, cleared in xylene for 5 minutes then mounted.

b) GFAP: ***(Carotti et al, 2008)***

Sections on coated slides were deparaffinized in xylene then taken through ethanol and rinsed in tap water to rehydrate. Endogenous peroxidase activity was blocked by incubating the sections in a solution of 3% hydrogen peroxide for 20 minutes at room temperature. Sections were immersed in antigen retrieval solution then washed with PBS for blocking of nonspecific protein binding. Sections were incubated with the diluted primary monoclonal anti rat-GFAP (1:100) at 4°C overnight using PBS at different dilutions for biotinylated secondary antibody. The sections were incubated for 30 minutes at room temperature with the appropriate secondary biotinylated antibody labeled with the avidin-biotin complex then washed with PBS for 5 minutes. The sections were developed with 3-DAB containing 1% hydrogen peroxide counterstained with Mayer's hematoxylin. Sections were rinsed in running tap water for 2-5 minutes, dehydrated through 95% ethanol for 1 minute and 100% ethanol for 3minutes, cleared in xylene for 5 minutes then mounted.

B- Oil Red O (ORO) staining: ***(Mehlem et al., 2013)***

Fresh liver samples was fixed in 10% neutral buffered formalin at 4 °C for two days and transferred to a 20% sucrose solution for two days then frozen. Frozen tissues were sectioned at 8-10 um on a cryostat then air dried. 1 ml of ORO working solution was added to cover the sections then incubated with ORO working solution at room temperature for 5 minutes. The sections were counterstained with Mayer's hematoxylin to visualize nuclei and tissue morphology. The sections were rinsed under running tap water for 30 minutes then mounted with glycerin jelly and covered with a cover slip.

2.4.5. Statistical analysis: ***(Hassan et al., 2018)***

Statistical analyses were performed, coded then analyzed using the computer program SPSS (Statistical package for social science) version 21.0. (Chicago, Illinois, USA). All data (body weight, TC, TG, ALT and AST) for all subgroups were expressed as mean ± standard deviation (SD). Intergroup differences were analyzed using analysis of variance (ANOVA) followed by post-hoc Scheffe test for multiple comparisons. All graphic representations of the data were performed with Microsoft® Excel® for windows®. (Microsoft Inc., USA).

3. Results

3.1. Gross examination of liver:

After sacrifaction, the liver extracted from the control groups (subgroup Ia and Ib) appeared dark red with smooth outlines. Livers of subgroup IIa were enlarged and yellowish in color. Livers obtained from subgroups IIb and IIc were red□brownish with smooth surfaces.

3.2. Rat body weight:

Control group (subgroup Ia & Ib):

There was no statistically significant difference between the mean body weight (WT) of subgroup Ia and subgroup Ib, therefore they were pooled into one group (control).

Experimental group (II):

All experimental subgroups (subgroup IIa, IIb and IIc) showed a highly significant increase in the mean body WT as compared to the control group. Both subgroups IIb and IIc showed a significant decrease in the mean body WT as compared to subgroup IIa. There was a nonsignificant difference in the mean body WT between subgroup IIb and subgroup IIc.

3.3. Biochemical results:

There was no statistically significant difference between the mean serum lipids and liver enzymes of subgroup Ia (negative control) and subgroup Ib (SE control), therefore they were pooled into one group (control)

3.3.1. serum lipids:

1) Serum triglyceride (TG):

Experimental group (II)*:*

All experimental subgroups (IIa, IIb and IIc) showed a highly significant increase in mean serum level of TG as compared to the control group. Regarding subgroups IIb and IIc, there was a

significant decrease in the mean serum level of TG as compared to subgroup IIa. There was a non-significant difference between subgroup IIb and subgroup IIc in the mean serum level of TG.

2) Serum total cholesterol (TC):

Experimental group (II)*:*

All experimental subgroups (IIa, IIb and IIc) showed a highly significant increase in mean serum level of TC as compared to the control group. Concerning subgroups IIb and IIc, there was a significant decrease in the mean serum level of TC as compared to subgroup IIa. There was a non-significant difference between subgroup IIb and subgroup IIc in the mean serum level of TC.

3.3.2. Liver enzymes:

As regards liver enzymes, subgroup IIb showed a significant reduction in the mean serum levels of ALT and a highly significant reduction of AST as compared to subgroup IIa. Subgroup IIc showed a highly significant reduction in the mean serum levels of ALT and AST as compared to subgroup IIa. On the other hand, subgroup IIc showed a significant decrease in the mean serum level of ALT enzyme as compared to subgroup IIb.

3.4. Histological results:

Examination of the liver sections of adult albino rats of subgroup Ia (negative control) and subgroup Ib (SE control) showed the same histological features.

3.4.1. Hematoxylin and Eosin stain (Hx. & E.):

Control group: Liver sections of this group showed the normal hepatic architecture formed of hexagonal hepatic lobules into which hepatic cords were radiated from central vein and separated by hepatic sinusoids. The hepatic cords consisted of polyhydral hepatocytes with rounded vesicular nuclei and granular eosinophilic cytoplasm. These cords formed pericentral zone around the central vein and periportal zone around the portal tract and midzonein between. Hepatic sinusoids were lined with endothelial cells and Kupffer cells while the portal tract consisted of a branch of; portal vein, hepatic artery and bile ductule.

Experimental group (II):

Subgroup IIa:

Examination of liver sections after 10 weeks of HFD showed loss of normal hepatic architecture with disturbed arrangement of hepatic cords and congested central veins while sinusoids were compressed by ballooned hepatocytes. Large lipid vacuoles filling the cytoplasm and pushing the nucleus to the periphery (macrovesicularsteatotic cells) as well as small fat droplets within the cytoplasm (microvesicularsteatotic cells) were seen in all zones of hepatocytes. The hepatocyte nuclei lost their vesicular appearance and became dark and small while clusters of inflammatory cells were infiltrating the portal tract. Mallory-Denk bodies were detected as irregular eosinophilic aggregates within the cytoplasm of some ballooned hepatocytes.

Subgroup IIb:

Liver sections showed moderate improvement and restoration of the hepatic architecture with cords of hepatocytes were radiating from central vein and separated by sinusoids which were lined with Kupffer cells. The normal hepatocytes appeared as polyhedral cells with granular eosinophilic cytoplasm and rounded vesicular nuclei, but large fat vacuoles pushed nucleus to the periphery in some hepatocytes.

Subgroup IIc:

Liver sections showed marked improvement of the hepatic architecture in the form of regular cords of hepatocytes radiating from central vein and separated by hepatic sinusoids which were lined with Kupffer cells. The hepatocytes appeared as polyhedral cells with granular eosinophilic cytoplasm and rounded vesicular nuclei. However, small fat droplets were present within the cytoplasm of some hepatocytes around central vein.

3.4.2. Mallory's trichrome stain:

Liver sections of this group showed normal architecture of liver with very faint collagen fibers around the central vein. Faint collagen fibers were present around the portal tract and between hepatocytes. Liver section in subgroup IIa showed extensive increase of collagen fibers around the central vein and portal tract that extended between the hepatocytes as compared to control group. Subgroup IIb showed decreased collagen fibers around the central vein, portal tract, between hepatocytes and around sinusoid while subgroup IIc showed few collagen fibers around central vein and portal tract as compared to subgroup IIa**.**

3.4.3. Immunohistochemical results:

a) TNF-α: TNF-α stained liver section of the control group showed negative TNF-α reaction within cytoplasm of hepatocytes.

Liver section of subgroups IIa showed highly increased number of TNF-α positive cells. Few number of TNF-α positive cells were detected in subgroup IIb, while subgroup IIc showed very few number of TNF-α positive cells as compared to subgroup IIa.

b) GFAP Stain:

GFAP section of the control group showed some brown stained star-shaped GFAP positive hepatic stellate cells. In comparison with control group, liver section of subgroups IIa showed markedly increased brown stained GFAP positive hepatic stellate cells. As compared to subgroup IIa, subgroup IIc showed reduced brown stained GFAP positive hepatic stellate cells, while subgroup IIc showed few GFAP positive hepatic stellate cells.

3.4.4. Oil Red O (ORO) stain:

ORO stained liver sections of the control group showed tiny red stained fat droplets within cytoplasm of hepatocytes. Liver section of subgroups IIa showed large distribution of multiple variable sized red stained fat droplets. Few red stained fat droplets were detected in subgroup IIb while subgroup IIc showed very few red stained fat droplets.

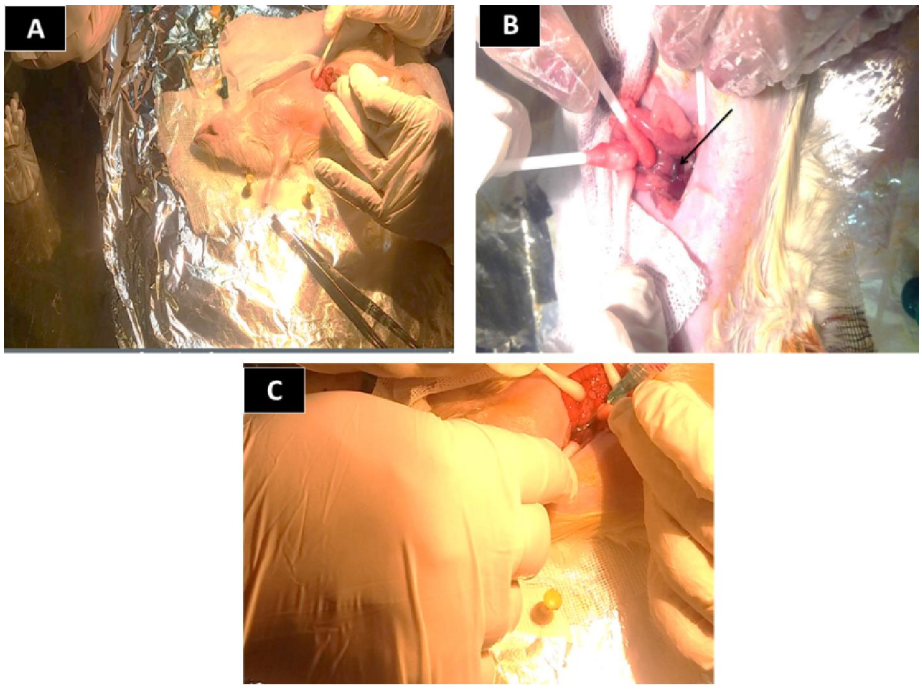

Fig. 1: A; Median abdominal incision into a rat of subgroup IIc. **B;** Identification of the portal vein (arrow). **C;** Intraportal injection of MSCs.

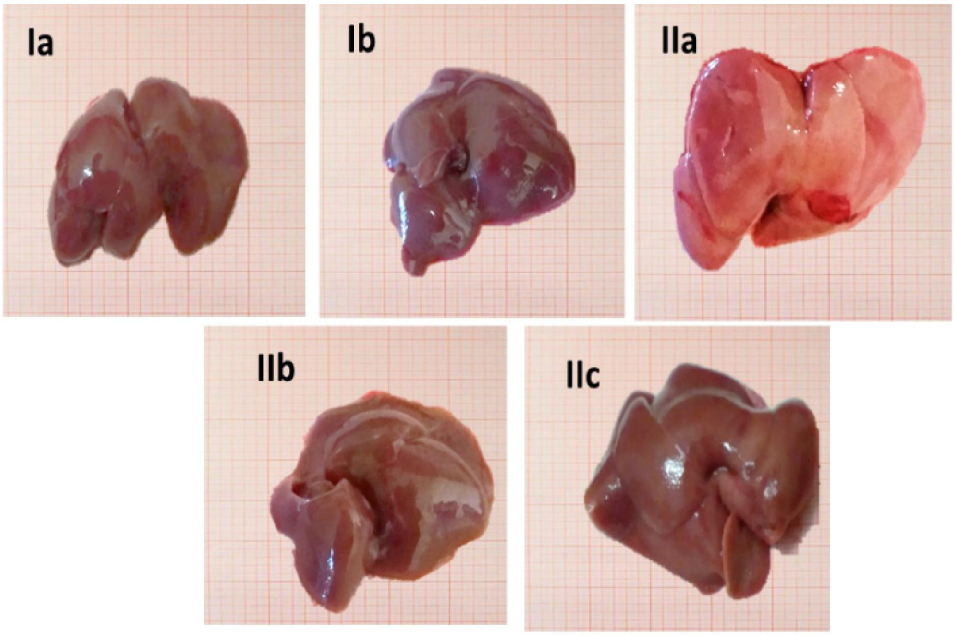

Fig. 2: Liver extracted from the control groups (subgroup Ia and Ib) appeared dark red with smooth outlines. Livers of subgroup IIa were enlarged and yellowish in color. Livers obtained from subgroups IIb and IIc were red-brownish with smooth surfaces.

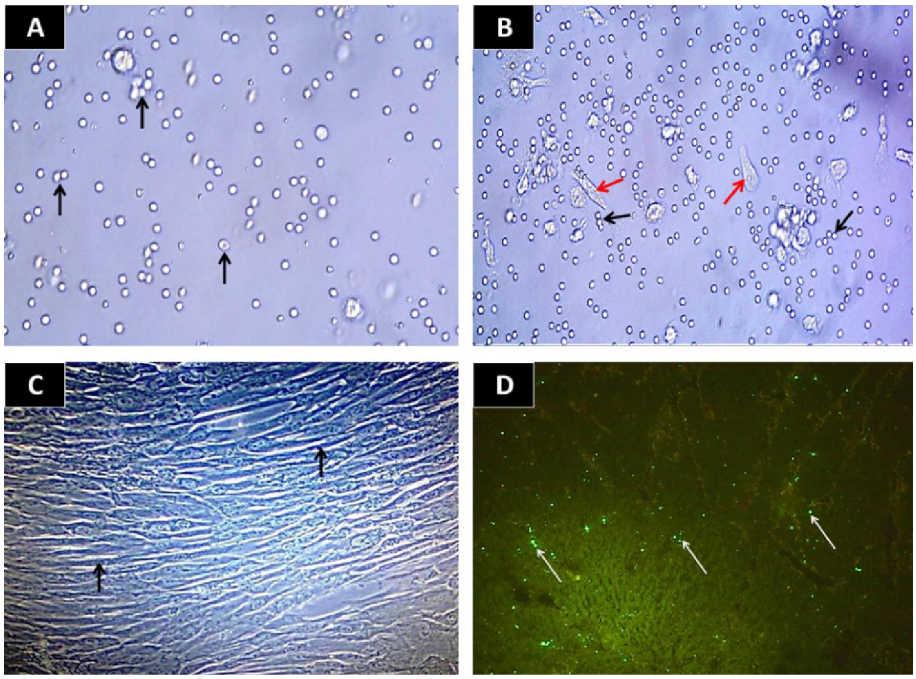

Fig. 3: A Photomicrograph of a primary culture of bone marrow derived mesenchymal stem cells at the 2nd day showing separated rounded cells of different size and arrangement (arrows). At the 6th day showing cells were crowded arranged either separately or in short chains (black arrows) while others are elongated (red arrows). **C);** Crowded spindle-shaped fibroblastic-like cells (arrows) appeared at the 14th day of primary culture. **D);** Fluorescence tracked GFP-labeled BM-MSCs of subgroup IIc appeared as green fluorescent dots (arrows). **(Inverted microscope; x40, x40, x100, Fluorescence microscope; x200)**

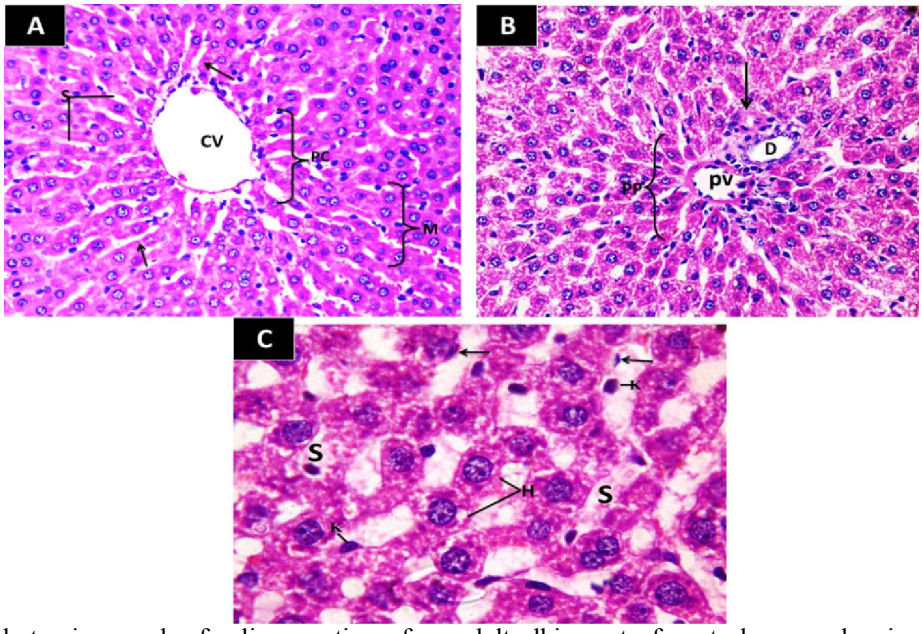

Fig. 4: A) A photomicrograph of a liver section of an adult albino rat of control group showing hepatic cords (arrows) radiating from the central vein (CV) and separated by the hepatic sinusoids (S). Notice pericentral zone (PC) and midzone (M) hepatocytes. **B);** portal tract consists of a branch of; portal vein (p), hepatic artery (arrow) and bile ductule (D) and surrounded by periportal (PP) zone of hepatocytes. **C);** polyhydral hepatocytes (H) appear with rounded vesicular nuclei and granular eosinophiliccytoplasm separated by sinusoids (S) which are lined with endothelial cells (arrows) and Kupffer cells (K). **(Hx. & E.; x400, x400, x1000)**

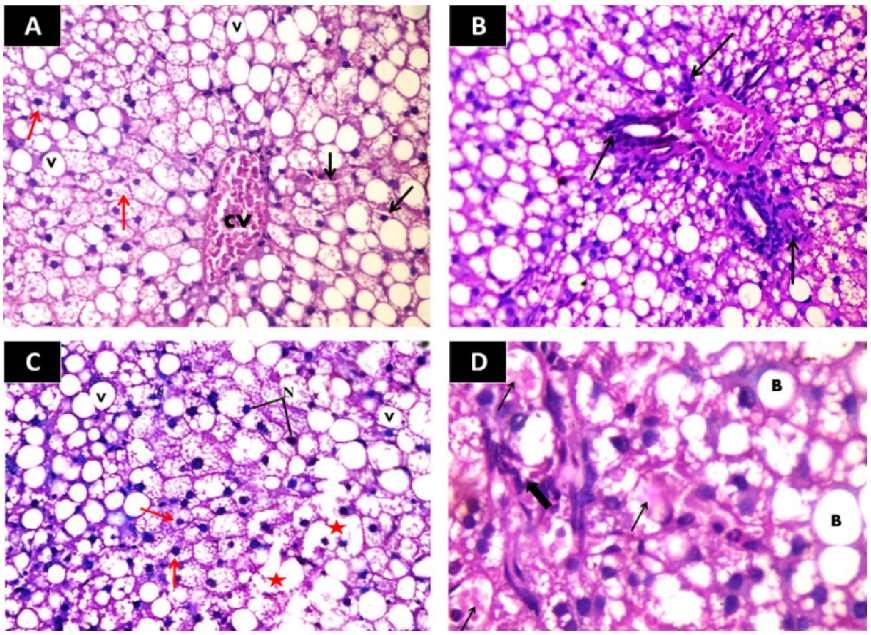

Fig. 5: A) A photomicrograph of a liver section liver section of an adult albino rat of subgroup IIa showing loss of normal architecture with congested central vein (CV). Widely distributed large lipid vacuoles (V), small fat droplets (red arrows). Notice compressed hepatic sinusoids (black arrows). **B);** inflammatory cells (arrows) are present around the three components of portal tract. **C);** The hepatocytes nuclei (N) appear dark pushed to one side and small with loss of their vesicular appearance. Notice multiple large lipid vacuoles (V) and small fat droplets (red arrows) with coalescence of multiple fat loculi (stars). **D);** Mallory-Denk bodies (thin arrows) appear as irregular shaped eosinophilic aggregates inside the cytoplasm of hepatocytes. Ballooned hepatocytes (B) and inflammatory cells (thick arrow) can be seen. **(Hx. & E.; x400, x400, x400, x1000)**

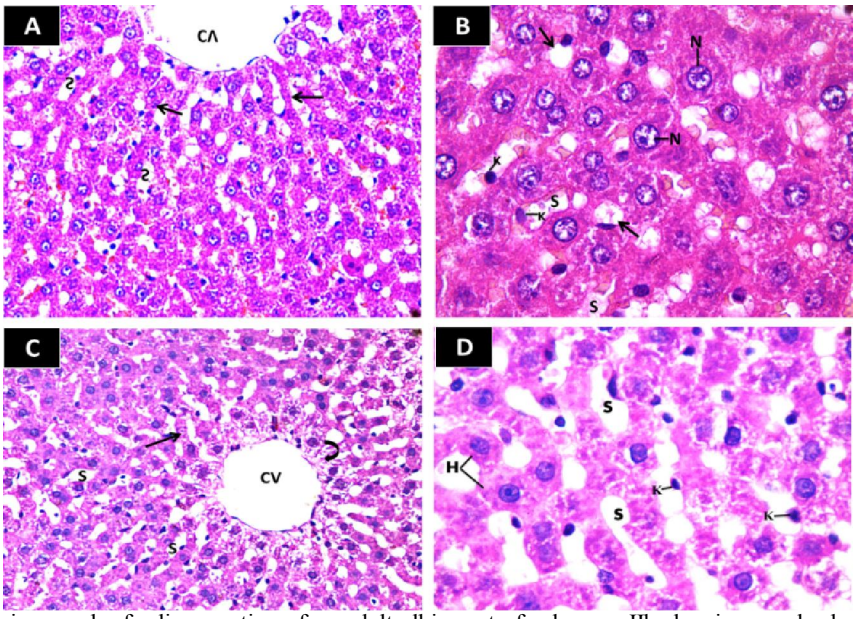

Fig. 6: A) A photomicrograph of a liver section of an adult albino rat of subgroup IIb showing regular hepatic cords (arrows) radiating from central vein (CV) and separated by sinusoids (S). **B);** Apparent normal hepatocytes with rounded vesicular nuclei (N) and granular eosinophilic cytoplasm separated by sinusoids (S) which are lined with Kupffer cells (K). Some hepatocytes (arrows) show large fat vacuoles pushing nucleus to the periphery. **(Hx. C);** A photomicrograph of a liver section of an adult albino rat of subgroup IIc showing regular cords (arrow) of hepatocytes radiating from central vein (CV) and separated by sinusoids (S). Small fat droplets (curved arrow) are present within the cytoplasm of pericentral zone hepatocytes. **D);** Hepatocytes (H) appear with round vesicular nuclei and eosinophilic granular cytoplasm and separated by sinusoids (S) which are lined with kupffer cells (K). **(Hx. & E.; x400, x1000, x400, x1000)**

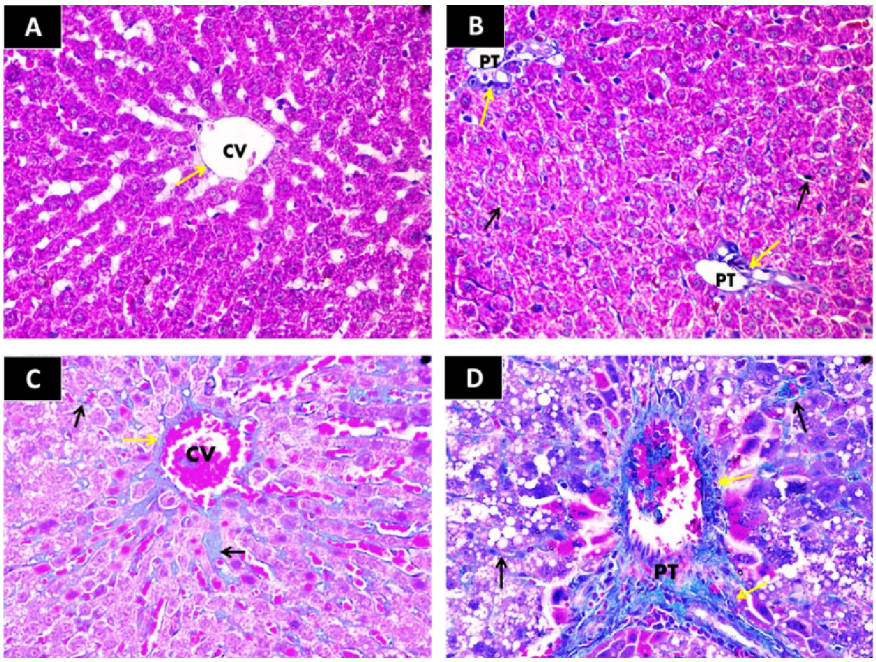

Fig. 7: A) A photomicrograph of a liver section of an adult albino rat of control group showing very faint collagen fibres (yellow arrow) around central vein (CV). **B);** Faint collagen fibres (yellow arrows) are present around portal tract (PT) and between hepatocytes (black arrows). **C);** A photomicrograph of a liver section of an adult albino rat of subgroup IIa showing obvious increase of collagen fibers (yellow arrow) around central vein (CV) extending between the hepatocytes and within sinusoids (black arrows). **D);** Extensive collagen fibers (yellow arrows) present around portal tract (PT) extending between the hepatocytes and within sinusoids (black arrows). **(Mallory's trichrome; x400)**

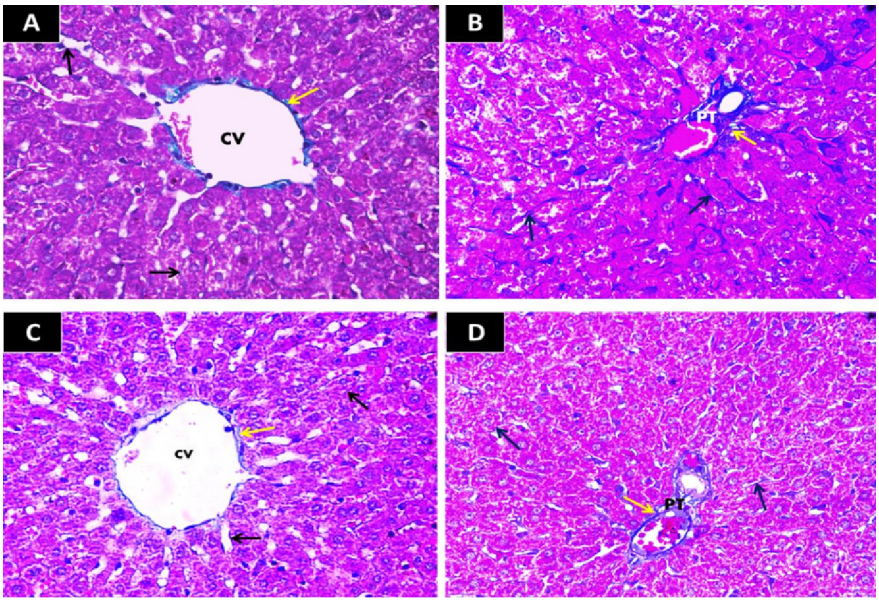

Fig. 8: A) A photomicrograph of a liver section of an adult albino rat of subgroup IIb showing decreased collagen fibers (yellow arrow) around the central vein (CV), between hepatocytes and within sinusoids (black arrows). **B);** Decreased collagen fibers (yellow arrow) around the portal tract (PT), between hepatocytes and within sinusoid (black arrows) as compared to subgroup IIa. **C);** Subgroup IIc showing few collagen fibers (yellow arrow) around the central vein (CV), between hepatocytes and within sinusoid (black arrows). **D);** Few collagen fibers (yellow arrow) around the portal tract (PT), between hepatocytes and within sinusoids (black arrows). **(Mallory's trichrome; x400)**

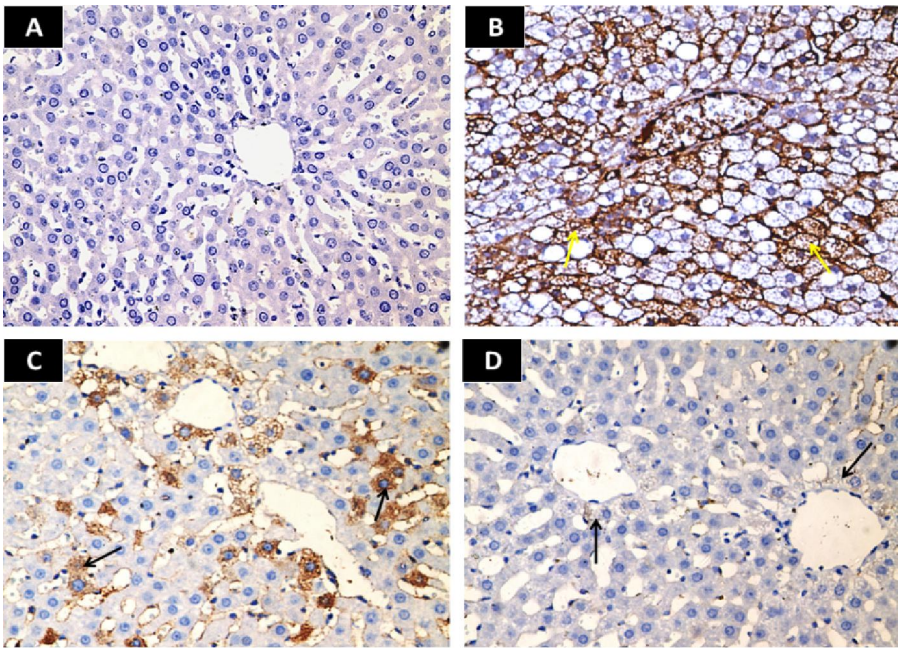

Fig. 9: A) A photomicrograph of a liver section of an adult albino rat of control group showing negative TNF-α reaction within cytoplasm of hepatocytes. **B);** Subgroup IIa showing marked increase in TNF-α positive cells (yellow arrows) in the form of brown stain within the cytoplasm of hepatocytes. **C);** Decreased number of TNF-α positive cells (arrows) in subgroup IIb as compared to subgroup IIa. **D);** Subgroup IIc showing very few TNF-α positive cells (arrows) **(Immunohistochemistry TNF-α.; x400)**

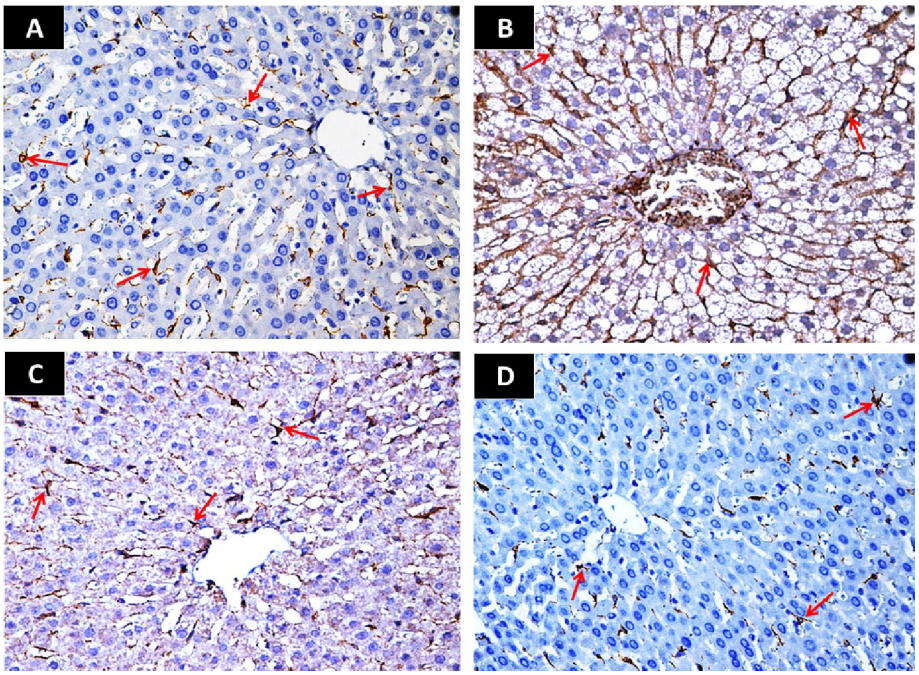

Fig. 10: A) A photomicrograph of a liver section of an adult albino rat of control group showing some GFAP positive hepatic stellate cells (red arrows) as brown stained star-shaped cells in the pericentral zone and mid zone. **B);** Subgroup IIa showing marked increase of brown stained GFAP positive hepatic stellate cells (red arrows). **C);** Subgroup IIb showing decreased brown stained GFAP positive hepatic stellate cells (red arrows). **D);** Subgroup IIc showing few GFAP +ve hepatic stellate cells (red arrows) as compared to subgroup IIa. **(Immunohistochemistry GFAP; x400)**

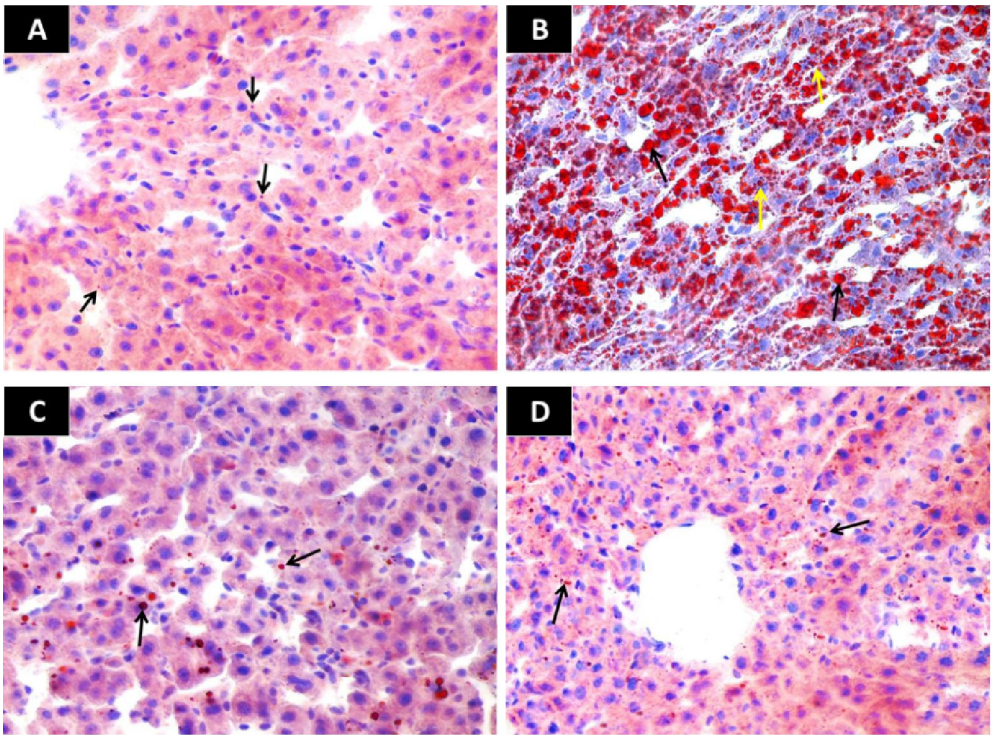

Fig. 11: A) A photomicrograph of a liver section of an adult albino rat of control showing tiny red stained fat droplets within hepatocytes. **B);** Subgroup IIa showing multiple small (yellow arrows) and large sized (black arrows) red stained fat droplets distributed in the section. **C);** Subgroup IIb showing few red stained fat droplets (arrows). **D);** Subgroup IIc showing very few red stained fat droplets (arrows) as compared to subgroup IIa. **(Oil Red O x400)**

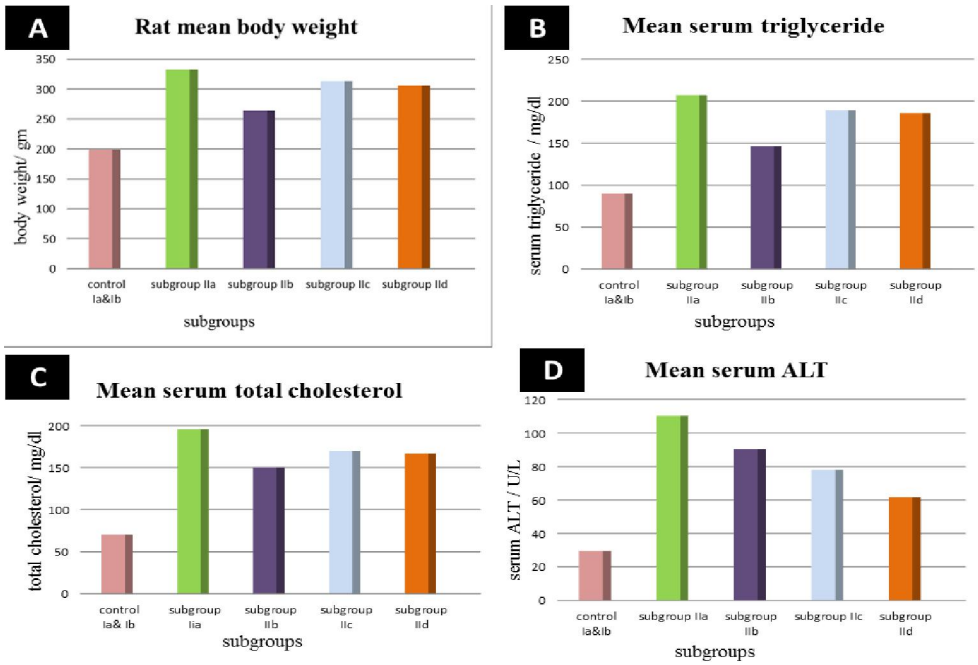

12: A) Comparison between the mean body weight (gm) in the different subgroups. **B)** Comparison between the mean serum level of TG (mg/dl) in the different subgroups. **C)** Comparison between the mean serum level of TC (mg/dl) in the different subgroups. **D)** Comparison of the mean serum ALT enzyme (U/L) in the different subgroups.

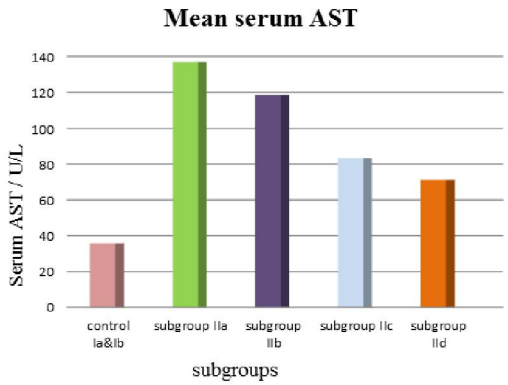

13: Comparison of the mean serum AST enzyme (U/L) in the different subgroups

4. Discussion

In the present work, livers extracted from control group had red, smooth and shiny appearance, but livers of subgroup IIa appeared enlarged and yellowish in color. This was in agreement with ***Liao et al. (2016)*** who stated that livers from NAFLD rats exhibited typical signs of hepatic steatosis with more yellow and rough surfaces compared with the livers from the normal rats.

In the current study, feeding rats of subgroup IIa high fat diet (HFD) for 10 weeks had produced obesity and NAFLD which was proved by increase of body weight, elevated serum levels of TG, TC and liver enzymes as well as decreased HDL. This result was in accordance with ***Ito et al. (2007)*** who mentioned that excess supply of free fatty acids directly via intake of HFD brought about triglyceride accumulation in the liver. Moreover, ***Gauthier et al. (2006) & Van Herck et al. (2017)*** stated that liver lipid content increased rapidly by approximately 200% during the first 2 weeks, decreased between weeks 2 and 6 then re-increased after 6 weeks in HFD rats. They added that, HFD had produced a phenotype similar to the human NAFLD characterized by obesity, insulin resistance and hyperlipidemia after 10 weeks.

Furthermore, the increased levels of liver enzymes in subgroup IIa were an indicator of hepatic damage. This was in agreement with ***Vernon et al. (2011) & Sanyal et al. (2015)*** who mentioned that NAFLD could be the most common cause of chronically elevated liver enzymes. They added that AST and ALT could be useful measures of NAFLD and were often the tipping point for further diagnostic evaluation. Moreover, ***Li et al. (2015) & Ma et al. (2017)*** stated that HFD induced imbalance of serum lipid and liver enzymes in rats. ***Khalil et al. (2018)*** added that the significant increase in levels of serum TC and TG were associated with the grade of NAFLD.

On the contrary, previous studies performed by ***Mofrad et al. (2003) & Fracanzani et al. (2008)*** detected that the entire histologic spectrum of NAFLD were seen in individuals with normal ALT values and this spectrum was not significantly different from those with elevated ALT levels. They added that a low normal ALT value did not guarantee freedom from underlying steatohepatitis with advanced fibrosis. ***Kälsch et al. (2015)*** stated that although the classic liver serum parameters (ALT and AST) were elevated in most chronic and acute liver diseases, they may not be ideal markers for liver injury in NAFLD.

In the present work, subgroup IIb and IIc showed a significant improvement of body weight, serum lipids and liver enzymes as compared to subgroup IIa. However, subgroup IId showed a significant decrease in the mean serum level of ALT and AST enzyme as compared to subgroup IIc.

The reduction of serum TG and TC in subgroup IIb could be explained according to ***Kushak et al. (2000); Ku et al. (2013) & Sanaei et al. (2015)*** who reported that AFA and blue green algea (BGA), from which SE is derived, inhibited intestinal lipid absorption and decreased plasma TC and TG concentrations suggesting that SE promoted lipid metabolism. Moreover, the decrease of liver enzymes in this subgroup was in accordance with ***Osman (2016)*** who stated that AST and ALT enzyme values were significantly decreased in the cirrhotic rats treated with SE and returned to the normal levels comparable to that of the control rats.

Furthermore, the improvement detected in subgroup IIc was in agreement with ***Liao et al. (2016)*** who reported that four weeks post-transplantation of adipose derived MSCs, body weight was decreased and the levels of lipid metabolism of rats with NAFLD were close to normal rats. They added that the serum levels of liver enzymes was significantly lowered in MSCs treated rats proving that MSCs transplantation accelerated the recovery of the liver from NAFLD progression.

In the current work, Hx. & E. stained liver sections of subgroup IIa showed loss of normal hepatic architecture with disturbed hepatic cords, steatosis and congested central and portal veins. Steatosis was in the form of macrovesicular type where large droplets nearly filled the whole cytoplasm pushing the nucleus to the periphery and microvesicular type where the cytoplasm was replaced by multiple small vacuoles giving the cell a foamy appearance. These findings were mentioned by ***Nalbantoglu and Brunt (2014) & Bedossa (2016)*** in their description of the histopathological pattern of NAFLD.

Moreover, this subgroup showed that steatosis was widely distributed in all hepatic zones with

numerous red stained lipids of variable size were observed in Oil Red O (ORO) sections. These results were confirmed by ***Fakhoury-Sayegh et al. (2015) & Song et al. (2017)*** whose histopathological observation using Hx. & E. and ORO staining revealed severe hepatic steatosis in rats fed with high fat diet.

On the contrary, ***Wree et al. (2014)*** reported that steatosis was mainly in the pericentral zone in NAFLD. However, ***Brown and Kleiner (2016)*** mentioned that early in the disease course, steatosis was most prominent in pericentral zone, but on progression of disease, steatosis could spread throughout the hepatic acinus or became irregularly distributed.

Leite et al. (2014) explained the occurrence of hepatic steatosis due to the disturbed balance between delivery, metabolism and synthesis of free fatty acids. Moreover, accumulation of lipids exerted toxic effects on the liver by inefficient oxidation or activation of inflammatory pathway. Similarly, ***Panqueva (2014) & Hassan et al. (2018)*** stated that microvesicular steatosis was associated with defective beta-oxidation of fatty acids including mitochondrial injury due oxidative stress that damage cell membrane as well as membranes of cell organelles. This damage led to increase in their permeability and disturbance of the ions concentrations in the cytoplasm and cell organelles.

In this experimental study, Hx. & E. stained liver sections of subgroup IIa, exhibited local inflammatory cellular infiltration around the portal tract. On the contrary, ***Argo et al. (2009) & Brunt (2010)*** observed that inflammation in NASH was often lobular and more prominent than portal inflammation in uncomplicated cases. However, ***Gadd et al. (2014)*** mentioned that portal inflammation became prominent in severe histologic injury and fibrosis suggesting that portal inflammation indicated worse prognosis.

In addition, this subgroup showed also markedly compressed hepatic sinusoids and ballooned hepatocytes with some having eosinophilic masses called Mallory-Denk Bodies (MDBs). Similar findings were observed by ***Lackner et al. (2008); Caldwell et al. (2010) & Kleiner and Makhlouf (2016)*** who defined ballooned hepatocytes by having a clear flocculent cytoplasm with a ballooned shape due to loss of their sharp angles and added that MDBs were considered as a marker of the progression of NASH. They explained the pathophysiological triggers of cytoplasmic ballooning due to damage of the intracellular intermediate filaments generated from metabolism of free fatty acids and fat accumulation in the endoplasmic reticulum of ballooned hepatocytes. Furthermore, ***Caldwell and Lackner (2017)*** added that the sinusoidal lumen was mechanically compressed by enlarged fat-laden hepatocytes in NAFLD.

Regarding Hx. & E. liver sections of subgroup IIb showed regular hepatic cords with large fat vacuoles in some hepatocytes and few red stained fat droplets. ***Drapeau et al. (2001), Benedetti et al. (2004) & Ku et al. (2013)*** explained reduced steatosis in subgroup IIb that AFA contains phycocyanin, carotenoids, minerals and vitamins C, E and B_{12} that function as antioxidants being beneficial for improving lipid metabolism.

On the other hand, subgroup IIc showed restored regular hepatic architecture with small fat droplets within hepatocytes of pericentral zone and very few ORO stained droplets as compared to subgroup IIa. The decrease of steatosis in subgroup IIc was explained by ***Pan et al. (2015) & Liao et al. (2016)*** who concluded that MSCs transplantation could enhance the reversion of NAFLD since lipid accumulation almost returned to normal levels in the MSCs-treated group. Moreover, ***Wang et al. (2017)*** reported that four weeks after MSCs transplantation, low grade-steatosis was observed and added that MSCs attenuated the development of NAFLD in mice by reduction of weight gain, hepatic steatosis, hepatocyte ballooning, liver inflammation and fibrosis.

In this experimental study, Mallory trichrome stained liver sections in subgroup IIa (10 weeks HFD) showed extensive collagen fibres around both central veins and portal tract and extended between hepatocytes in comparison with control groups. This was in agreement with ***Brown and Kleiner (2016)*** who stated that fibrosis was often present in NASH and usually consisted of perisinusoidal/pericellular fibrosis giving a chicken wire pattern. However, portal fibrosis could be seen as the severity of disease increased and untreated cases would progress to bridging fibrosis and cirrhosis.

Fibrosis, in this study, was also confirmed by glial fibrillary acidic protein (GFAP) immunostain for detection of hepatic stellate cells, where subgroup IIa showed marked increase in GFAP positive hepatic stellate cells. This results was in agreement with ***Hassan et al. (2018)*** who revealed that NAFLD rats showed strong positive immune expression of hepatic stellate cells markers (GFAP) in comparison with the control rats.

Kim et al. (2018) explained that hepatic fibrosis in NASH was usually initiated by hepatocytes damage leading to activation of kupffer cells and subsequent release of cytokines and growth factors. These factors activated hepatic stellate cells which proliferated and changed from the star-shaped stellate cells to myofibroblasts like cell synthesizing a large amount

of extra cellular matrix components including collagen, proteoglycan and adhesive glycoproteins.

Concerning subgroup IIb, it showed a decrease of collagen fibers as well as reduction of brown stained GFAP positive hepatic stellate cells as compared to subgroup IIa. However, this reduction was in a little degree as compared to subgroup IIc. In agreement with these findings ***El-Akabawy and El-Mehi (2015) & Osman (2016)*** proved that SE caused reduction in collagen fibers and reverse fibrogenesis in a Thioacetamide induced liver fibrosis.

In the present study, subgroup IIc exhibited few collagen fibres in addition to few GFAP positive hepatic stellate cells as compared to subgroup IIa. These results were concluded by ***Zhao et al. (2005) & Rabani et al. (2010)*** who stated that collagen accumulation and fatty degeneration were significantly decreased after four weeks of BM-MSCs transplantation in carbon tetrachloride induced liver fibrosis in rats. They added that the thickened septal fibrosis became thinner. Furthermore, ***Wang et al. (2017)*** coincided the results of this study and demonstrated the ability of mesenchymal stem cells to significantly reverse liver fibrosis and attenuate nonalcoholic steatohepatitis in mice.

Zhang et al. (2018) & Li et al. (2019) also reported that MSCs played an inhibitory role in the process of hepatic stellate cells transition from the quiescent state to activated state and their apoptosis through release of interleukin-1. They also proved that BM-MSCs reduced expression of collagen type I.

In this study, TNF-α immunostaining revealed a highly increased number of TNF-α positive cells in subgroup IIa (10 weeks HFD) as compared to the control group which negatively expressed it. This result was explained by ***Braunersreuther et al. (2012)*** who stated that TNF-α production was due to oxidative stress which led to the production of proinflammatory cytokines. Moreover, ***Henriques et al. (2014)*** mentioned that TNF-α was considered to be a major inflammatory mediator of steatosis, insulin resistance and associated with inflammatory disorders liver fibrosis.

Kim (2012) & Ajmal et al. (2014) added that TNF-α played a key role in the progression of NAFLD to NASH inducing necrosis and angiogenesis. Furthermore, in high concentrations, TNF-α suppressed cell development and produced lipogenic and fibrogenic effects involving activation of Kupffer cells with the release of soluble mediators which stimulated the transformation of hepatic stellate cells into myofibroblasts.

In the present study, subgroups IIb and IIc showed a highly significant decrease in the mean number of TNF-α positive cells as compared to subgroup IIa.

These finding were in agreement with ***El-Akabawy and El-Mehi (2015) & Osman (2016)***, who reported that using SE on a thioacetamide induced liver injury, downregulated the TNF-α expression in affected animals and improved the histopathological changes of fibrosis. On the other hand, ***Ezquer et al. (2017)*** proved that TNF-α was markedly decreased in NAFLD obese mice that were treated with MSCs. Similarly, ***El‐Tahawy and Ali (2017)*** stated that administration of BM-MSCs normalized the over expression of TNF-α in injured liver tissues.

In the current study, as regard subgroup IIc, GFP labelled BM-MSCs were detected in the liver section by fluorescent microscope four weeks after intraportal transplantation. ***Song et al. (2015)*** agreed this result and stated that the expression of GFP was visible in the livers of the rats transplanted with BM-MSCs via the portal vein indicating that BM-MSCs were able to colonize the liver.

On the other hand, ***Boeykens et al. (2013)*** explained the exact mechanism behind BM-MSCs retention in the liver following intraportal injection in GFP sections due to active homing leading to entrapment of injected BM-MSCs into the microcirculation of the liver.

Conclusion

The results of this study concluded that feeding rats with HFD for 10 weeks led to appearance of NASH which was proved by histological and biochemical results. On the other hand, mobilization of endogenous stem cells using Stem Enhance led to moderate improvement concerning weight, liver functions, hepatic fats and fibrosis.

BM-MSCs intraportal transplantation significantly improved liver function, promoted lipid metabolism and decreased the intrahepatic fibrosis and content of lipids thus reversing the progression of NAFLD. Therefore, exogenous BM-MSCs provide a better therapeutic approach for NASH as compared to mobilization of endogenous stem cells using Stem Enhance.

Acknowledgements

We are so grateful to all the research technicians at Tanta and Mansoura universities for their help and support throughout the project.

References

1. *Ajmal, M.R.; Yaccha, M.; Malik, M.A.; Rabbani, M.U.; Ahmad, I.; Isalm, N. and Abdali, N. (2014)*: Prevalence of nonalcoholic fatty liver disease (NAFLD) in patients of cardiovascular diseases and its association with hs-CRP and TNF-α. Indian heart journal; 66(6): 574-579.

2. *Argo, C.K.; Northup, P.G.; Al-Osaimi, A.M. and Caldwell, S.H. (2009)*: Systematic review of risk factors for fibrosis progression in non-alcoholic steatohepatitis. J Hepatol.; 51(2): 371-379.
3. *Bancroft, J.D. and Layton, C. (2013)*: The hematoxylin and eosin, Connective and mesenchymal tissues with their stains in: Suvarna KS, Layton C, Bancroft JD. Bancroft's theory and practice of Histological Techniques 7th ed. Chapter 10 & 11. Churchill Livingstone Elsevier Ltd, Philadelphia. Pp: 174-213.
4. *Bedossa, P. (2016)*: Histological assessment of NAFLD. Digestive diseases and sciences; 61(5): 1348-1355.
5. *Benedetti, S.; Benvenuti, F.; Pagliarini, S.; Francogli, S.; Scoglio, S. and Canestrari, F. (2004)*: Antioxidant properties of a novel phycocyanin extract from the bluegreen alga Aphanizomenonflos-aquae. Life Sciences; 75(19): 2353-2362.
6. *Boeykens, N.; Ponsaerts, P.; Van der Linden, A.; Berneman, Z.; Ysebaert, D. and De Greef, K. (2013)*: Injury-dependent retention of intraportally administered mesenchymal stromal cells following partial hepatectomy of steatotic liver does not lead to improved liver recovery. PLoS One; 8(7): e69092.
7. *Braunersreuther, V.; Viviani, G.L.; Mach, F. and Montecucco, F. (2012)*: Role of cytokines and chemokines in non-alcoholic fatty liver disease. World journal of gastroenterology: WJG; 18(8): 727-735.
8. *Brown, G.T. and Kleiner, D.E. (2016)*: Histopathology of nonalcoholic fatty liver disease and nonalcoholic steatohepatitis. Metabolism; 65(8): 1080-1086.
9. *Brunt, E.M. (2010)*: Pathology of nonalcoholic fatty liver disease. Nat Rev. Gastroenterol. Hepatol.; 7(4): 195-203.
10. *Caldwell, S. and Lackner, C. (2017)*: Perspectives on NASH histology: Cellular ballooning. Annals of hepatology; 16(2): 182-184.
11. *Caldwell, S.; Ikura, Y.; Dias, D.; Isomoto, K.; Yabu, A.; Moskaluk, C.; Pramoonjago, P.; Simmons, W.; Scruggs, H.; Rosenbaum, N. and Wilkinson, T. (2010)*: Hepatocellular ballooning in NASH. Journal of hepatology; 53(4): 719-723.
12. *Carotti, S.; Morini, S.; Corradini, S.G.; Burza, M.A.; Molinaro, A.; Carpino, G.; Merli, M.; De Santis, A.; Muda, A.O.; Rossi, M. and Attili, A.F. (2008)*: Glial fibrillary acidic protein as an early marker of hepatic stellate cell activation in chronic and posttransplant recurrent hepatitis C. Liver Transplantation; 14(6): 806-814.
13. *Drapeau, C.; Kushak, R.I.; Van Cott, E.M. and Winter, H.H. (2001)*:"Blue-green alga aphanizomenonflos-aquae as a source of dietary polyunsaturated fatty acids and a hypocholesterolemic agent." In ACS SYMPOSIUM SERIES; 788: 125-141.
14. *El-Akabawy, G. and El-Mehi, A. (2015)*: Mobilization of endogenous bone marrow-derived stem cells in a thioacetamide-induced mouse model of liver fibrosis. Tissue Cell.; 47(3): 257-265.
15. *El‐Tahawy, N. and Ali, A.H. (2017)*: Possible protective effect of bone marrow‐mesenchymal stem cells (BM‐MSCs) against the remote liver injury induced by renal ischemia reperfusion in male albino rats. Journal of Cytology & Histology; 8(484): 1-14.
16. *Ezquer, M.; Ezquer, F.; Ricca, M.; Allers, C. and Conget, P. (2017)*: Intravenous administration of multipotent stromal cells prevents the onset of non-alcoholic steatohepatitis in obese mice with metabolic syndrome. J. Hepatol.; 55(5): 1112-1120.
17. *Fakhoury-Sayegh, N.; Trak-Smayra, V.; Khazzaka, A.; Esseily, F.; Obeid, O.; Lahoud-Zouein, M. and Younes, H. (2015)*: Characteristics of nonalcoholic fatty liver disease induced in wistar rats following four different diets. Nutrition research and practice; 9(4): 350-357.
18. *Filozof, C.; Goldstein, B.J.; Williams, R.N. and Sanyal, A. (2015)*: Non-alcoholic steatohepatitis: Limited available treatment options, but promising drugs in development and recent progress towards a regulatory approval pathway. Drugs; 75(12):1373-1392.
19. *Fracanzani, A.L.; Valenti, L.; Bugianesi, E.; Andreoletti, M.; Colli, A.; Vanni, E.; Bertelli, C.; Fatta, E.; Bignamini, D.; Marchesini, G. and Fargion, S. (2008)*: Risk of severe liver disease in nonalcoholic fatty liver disease with normal aminotransferase levels: A role for insulin resistance and diabetes. Hepatology; 48(3):792-798.
20. *Fujimoto, M., Tsuneyama, K., Chen, S.Y., Nishida, T., Chen, J.L., Chen, Y.C., Fujimoto, T., Imura, J. and Shimada, Y. (2012)*: Study of the effects of monacolin k and other constituents of red yeast rice on obesity, insulin-resistance, hyperlipidemia, and nonalcoholic steatohepatitis using a mouse model of metabolic syndrome. Evidence-Based Complementary and Alternative Medicine: e892697.
21. *Gabr, H.; El-Kheir, W.A.; Farghali, H.A.; Ismail, Z.M.; Zickri, M.B.; Maadawi, Z.M.E.; Kishk, N.A. and Sabaawy, H.E. (2015)*: Intrathecal transplantation of autologous adherent bone marrow cells induces functional neurological recovery in a canine model of spinal cord injury. Cell transplantation; 24(9): 1813-1827.
22. *Gadd, V.L.; Skoien, R.; Powell, E.E.; Fagan, K.J.; Winterford, C.; Horsfall, L.; Irvine, K. and Clouston, A.D. (2014)*: The portal inflammatory infiltrate and ductular reaction in human nonalcoholic fatty liver disease. Hepatology; 59(4): 1393-1405.

23. *Gauthier, M.S.; Favier, R. and Lavoie, J.M. (2006)*: Time course of the development of non-alcoholic hepatic steatosis in response to high-fat diet-induced obesity in rats. British Journal of Nutrition; 95(2): 273-281.
24. *Goddard, E. T.; Fischer, J. and Schedin, P. (2016)*: A Portal Vein Injection Model to Study Liver Metastasis of Breast Cancer. Journal of Visualized Experiments; (118): e54903.
25. *Guo, Y.; Su, L.; Wu, J.; Zhang, D.; Zhang, X.; Zhang, G.; Li, T.; Wang, J. and Liu, C. (2012)*: Assessment of the green florescence protein labeling method for tracking implanted mesenchymal stem cells. Cytotechnology; 64(4): 391-401.
26. *Hassan, N.F.; Soliman, G.M.; Okasha, E.F. and Shalaby, A.M. (2018)*: Histological, immunohistochemical, and biochemical study of experimentally induced fatty liver in adult male albino rat and the possible protective role of pomegranate. Journal of Microscopy and Ultrastructure; 6(1): 44-55.
27. *Henriques, M.S., Leite, J.A., Diniz, M.D. and Araújo, M.S. (2014)*: Immunohistochemistry pattern of hepatic inflammatory and insulin resistance markers in experimental model of nonalcoholic steatohepatitis. Journal Brasileiro de Patologia e Medicina Laboratorial; 50(2): 136-143.
28. *Ismail, Z.M.; Kamel, A.M.; Yacoub, M.F. and Aboulkhair, A.G. (2013)*: The effect of in vivo mobilization of bone marrow stem cells on the pancreas of diabetic albino rats (a histological & immunohistochemical study). Int. J. Stem Cells; 6(1): 1-11.
29. *Ito, M.; Suzuki, J.; Tsujioka, S.; Sasaki, M.; Gomori, A.; Shirakura, T.; Hirose, H.; Ito, M.; Ishihara, A.; Iwaasa, H. and Kanatani, A. (2007)*: Longitudinal analysis of murine steatohepatitis model induced by chronic exposure to high‐fat diet. Hepatology Research; 37(1): 50-57.
30. *Kallis, Y.N.; Alison, M.R. and Forbes, S.J. (2007)*: Bone marrow stem cells and liver disease. Gut; 56(5): 716-724.
31. *Kälsch, J.; Bechmann, L.P.; Heider, D.; Best, J.; Manka, P.; Kälsch, H.; Sowa, J.P.; Moebus, S.; Slomiany, U.; Jöckel, K.H. and Erbel, R. (2015)*: Normal liver enzymes are correlated with severity of metabolic syndrome in a large population based cohort. Scientific reports; 5: 13058-13066.
32. *Karaoz, E.; Aksoy, A.; Ayhan, S.; Sariboyaci, A.E.; Kaymaz, F. and Kasap, M. (2009)*: Characterization of mesenchymal stem cells from rat bone marrow: Ultrastructural properties, differentiation potential and immunophenotypic markers. Histochemistry and Cell Biology; 132(5): 533-546.
33. *Khalil, F.; Rafat, M.N.; Salah, M.; Mohamed, M.A. and Ibrahim, W. (2018)*: Study of Lipid Profile in Different grades of Non-Alcoholic Fatty Liver Disease. The Egyptian Journal of Hospital Medicine; 73(8): 7388-7393.
34. *Kim, B.M.; Abdelfattah, A.M.; Vasan, R.; Fuchs, B.C. and Choi, M.Y. (2018)*: Hepatic stellate cells secrete Ccl5 to induce hepatocyte steatosis. Scientific reports; 8(1): 7499-7508.
35. *Kim, J.S. (2012)*: The role of inflammatory mediators in the pathogenesis of nonalcoholic fatty liver disease. Pediatric Gastroenterology, Hepatology & Nutrition; 15(2): 74-78.
36. *Kim, T.H.; Kim, J.K.; Shim, W.; Kim, S.Y.; Park, T.J. and Jung, J.Y. (2010)*: Tracking of transplanted mesenchymal stem cells labeled with fluorescent magnetic nanoparticle in liver cirrhosis rat model with 3-T MRI. Magnetic Resonance Imaging; 28(7): 1004-1013.
37. *Kleiner, D.E. and Makhlouf, H.R. (2016)*: Histology of nonalcoholic fatty liver disease and nonalcoholic steatohepatitis in adults and children. Clinics in liver disease; 20(2): 293-312.
38. *Ku, C.S.; Yang, Y.; Park, Y. and Lee, J. (2013)*: Health benefits of blue-green algae: Prevention of cardiovascular disease and nonalcoholic fatty liver disease. J. Med. Food; 16(2): 103-111.
39. *Kushak, R.I.; Drapeau, C.; Van Cott, E.M. and Winter, H.H. (2000)*: Favorable effects of bluegreen algae Aphanizomenonflos-aquae on rat plasma lipids. J. Am. Nutraceutical Assoc.; 2(3): 59-65.
40. *Lackner, C.; Gogg-Kamerer, M.; Zatloukal, K.; Stumptner, C.; Brunt, E.M. and Denk, H. (2008)*: Ballooned hepatocytes in steatohepatitis: The value of keratin immunohistochemistry for diagnosis. Journal of hepatology; 48(5): 821-828.
41. *Lau, J.K.; Zhang, X. and Yu, J. (2016)*: Animal models of non-alcoholic fatty liver disease: current perspectives and recent advances. The Journal of pathology; 241(1): 36-44.
42. *Leite, N.C.; Villela-Nogueira, C.A.; Cardoso, C.R. and Salles, G.F. (2014)*: Non-alcoholic fatty liver disease and diabetes: from physiopathological interplay to diagnosis and treatment. World Journal of Gastroenterology. W.J.G.; 20(26): 8377-8392.
43. *Li, H.; Shen, S.; Fu, H.; Wang, Z.; Li, X.; Sui, X.; Yuan, M.; Liu, S.; Wang, G. and Guo, Q. (2019)*: Immunomodulatory Functions of Mesenchymal Stem Cells in Tissue Engineering. Stem cells international; 1-18.
44. *Li, L.; Li, L.; Chen, L.; Lin, X.; Xu, Y., Ren, J.; Fu, J. and Qiu, Y. (2015)*: Effect of oleoylethanolamide on diet-induced nonalcoholic fatty liver in rats. Journal of pharmacological sciences; 127(3):244-250.
45. *Liao, N.; Pan, F.; Wang, Y.; Zheng, Y.; Xu, B.; Chen, W.; Gao, Y.; Cai, Z.; Liu, X. and Liu, J. (2016)*: Adipose tissue-derived stem cells promote the reversion of non-alcoholic fatty liver disease: an in vivo study. International journal of molecular medicine; 37(5): 1389-1396.

46. *Loomba, R. and Sanyal, A.J. (2013)*: The global NAFLD epidemic. Nature reviews Gastroenterology & hepatology; 10(11): 686-690.
47. *Ma, Z.; Chu, L.; Liu, H.; Wang, W.; Li, J.; Yao, W.; Yi, J. and Gao, Y. (2017)*: Beneficial effects of paeoniflorin on non-alcoholic fatty liver disease induced by high-fat diet in rats. Scientific reports; 7: 44819-44828.
48. *McPherson, S.; Hardy, T.; Henderson, E.; Burt, A.D.; Day, C.P. and Anstee, Q.M., (2015)*: Evidence of NAFLD progression from steatosis to fibrosing-steatohepatitis using paired biopsies: Implications for prognosis and clinical management. Journal of hepatology; 62(5):1148-1155.
49. *Mehlem, A.; Hagberg, C.E.; Muhl, L.; Eriksson, U. and Falkevall, A. (2013)*: Imaging of neutral lipids by Oil red O for analyzing the metabolic status in health and disease. Nature protocols; 8(6):1149-1154.
50. *Nalbantoglu, I. and Brunt, E.M., (2014)*: Role of liver biopsy in nonalcoholic fatty liver disease. World Journal of Gastroenterology: W.J.G.; 20(27): 9026-9037.
51. *Osman, N. (2016)*: The stem cell mobilizer StemEnhance reduces fibrosis and enhances proliferation in Thioacetamide induced-liver cirrhosis in the adult male albino rat. European journal of anatomy; 20(1): 37-45.
52. *Pan, F.; Liao, N.; Zheng, Y.; Wang, Y.; Gao, Y.; Wang, S.; Jiang, Y. and Liu, X. (2015)*: Intrahepatic transplantation of adipose-derived stem cells attenuates the progression of non-alcoholic fatty liver disease in rats. Molecular medicine reports; 12(3): 3725-3733.
53. *Panqueva, R.P. (2014)*: Pathological aspects of fatty liver disease. Rev. Col. Gastroenterol.; 29(1): 72-78.
54. *Rabani, V.; Shahsavani, M.; Gharavi, M.; Piryaei, A.; Azhdari, Z. and Baharvand, H. (2010)*: Mesenchymal stem cell infusion therapy in a carbon tetrachloride‐induced liver fibrosis model affects matrix metalloproteinase expression. Cell biology international; 34(6):601-605.
55. *Sanaei, M.; Ebrahimi, M.; Banazadeh, Z.; Shafiee, G.; Khatami, F.; Ahadi, Z. and Heshmat, R. (2015)*: Consequences of Aphanizomenon Flos-aqua (AFA) extract (Stemtech TM) on metabolic profile of patients with type 2 diabetes. Journal of Diabetes & Metabolic Disorders; 14(1): 50-56.
56. *Sanyal, D.; Mukherjee, P.; Raychaudhuri, M.; Ghosh, S.; Mukherjee, S. and Chowdhury, S. (2015)*: Profile of liver enzymes in non-alcoholic fatty liver disease in patients with impaired glucose tolerance and newly detected untreated type 2 diabetes. Indian journal of endocrinology and metabolism; 19(5): 597-601.
57. *Song, L.; Qu, D.; Zhang, Q.; Zhou, H.; Jiang, R.; Li, Y.; Zhang, Y. and Yan, H. (2017)*: Phytosterol esters attenuate hepatic steatosis in rats with non-alcoholic fatty liver disease rats fed a high-fat diet. Scientific reports; 7: 41604-41621.
58. *Song, Y.M.; Lian, C.H.; Wu, C.S.; Ji, A.F.; Xiang, J.J. and Wang, X.Y. (2015)*: Effects of bone marrow-derived mesenchymal stem cells transplanted via the portal vein or tail vein on liver injury in rats with liver cirrhosis. Experimental and therapeutic medicine; 9(4): 1292-1298.
59. *Van Herck, M.; Vonghia, L. and Francque, S. (2017)*: Animal models of nonalcoholic fatty liver disease-a starter's guide. Nutrients; 9(10):1072-1084.
60. *Vernon, G.; Baranova, A. and Younossi, Z.M. (2011)*: Systematic review: The epidemiology and natural history of non-alcoholic fatty liver disease and non-alcoholic steatohepatitis in adults. Aliment. Pharmacol. Ther.; 34(3): 274-285.
61. *Wang, H.; Wang, D.; Yang, L.; Wang, Y.; Jia, J.; Na, D.; Chen, H.; Luo, Y. and Liu, C. (2017)*: Compact bone-derived mesenchymal stem cells attenuate nonalcoholic steatohepatitis in a mouse model by modulation of CD4 cells differentiation. International immunopharmacology; 42,: 67-73.
62. *Wang, Y.; Lian, F.; Li, J.; Fan, W.; Xu, H.; Yang, X.; Liang, L.; Chen, W. and Yang, J. (2012)*: Adipose derived mesenchymal stem cells transplantation via portal vein improves microcirculation and ameliorates liver fibrosis induced by CCl4 in rats. Journal of translational medicine; 10(1): 133-141.
63. *Wree, A.; Schlattjan, M.; Bechmann, L.P.; Claudel, T.; Sowa, J.P.; Stojakovic, T.; Scharnagl, H.; Köfeler, H.; Baba, H.A.; Gerken, G. and Feldstein, A.E. (2014)*: Adipocyte cell size, free fatty acids and apolipoproteins are associated with non-alcoholic liver injury progression in severely obese patients. Metabolism; 63(12): 1542-1552.
64. *Yusop, N.; Battersby, P.; Alraies, A.; Sloan, A.J.; Moseley, R. and Waddington, R.J. (2018):*Isolation and Characterization of Mesenchymal Stem Cells from Rat Bone Marrow and the Endosteal Niche: A Comparative Study. Stem cells international:1-35.
65. *Zhang, Y.; Li, Y.; Zhang, L.; Li, J. and Zhu, C. (2018)*: Mesenchymal stem cells: Potential application for the treatment of hepatic cirrhosis. Stem cell research & therapy; 9(1): 59-65.
66. *Zhang, Z. and Wang, F.S. (2013)*: Stem cell therapies for liver failure and cirrhosis. Journal of Hepatology; 59(1): 183-185.
67. *Zhao, D.C.; Lei, J.X.; Chen, R.; Yu, W.H.; Zhang, X.M.; Li, S.N. and Xiang, P. (2005)*: Bone marrow-derived mesenchymal stem cells protect against experimental liver fibrosis in rats. World journal of gastroenterology: W.J.G.; 11(22): 3431-3440.

11/30/2019